Results in Surfaces and Interfaces 16 (2024) 100242

Contents lists available at ScienceDirect

Results in Surfaces and Interfaces

journal homepage: www.elsevier.com/locate/rsurfi

NiFe based synthetic LDH, study of chromate adsorption mechanisms

Anna Maria Cardinale *, Marco Fortunato, Francisco Ardini

Department of Chemistry and Industrial Chemistry, University of Genoa, 16146, Genoa, Italy

ARTICLE INFO

Keywords:
NiFe-NO_3 LDH
Chromium (VI) removal
Experimental design
Adsorption mechanism
Cage effect

ABSTRACT

Layered Double Hydroxides (LDH) have proven to be extremely versatile compounds, suitable for multiple uses in different fields of technology. In this work, a NiFe–NO_3 LDH was synthesized, and its structure was confirmed by means of X-Ray Powder Diffraction (XRPD), FT-InfraRed Spectroscopy (FT-IR) and Field Emission Scanning Electron Microscopy (FE-SEM). The compound efficiency as adsorber of Cr(VI) in water solution was studied, planning the adsorption experiments through the use of the experimental design techniques (Design of Experiment – DOE). For the purpose to find a reuse of the LDH, after the chromium remediation process, according with the circular economy statements, the chromate capture mechanism was investigated. The results demonstrate that the chromate adsorption capacity is influenced mainly by the ratio LDH mass/solution volume and the initial concentrations of Cr(VI). As the adsorption mechanism, it consists of two different processes, the interlayer exchange and an entrapment of the chromate into the external octahedral sites of the layers.

1. Introduction

The layered morphology, coupled with the capacity to intercalate various anionic species (both inorganic and organic) in different compositions, arouses a growing interest in the possibility to apply LDHs in research fields that are very distant from each other. A particularly widespread application consists in the removal of contaminants or pollutants from water, whether civil, irrigation drainage and industrial waste, such as for example phosphates, chromates, selenate, surfactants and dyes (Cardinale et al., 2023; Thite and Giripunje, 2022; Lei et al., 2017; Zheng et al., 2019; Machrouhi et al., 2022; Li et al., 2019; Jiehu et al., 2020). Furthermore, the LDHs are applied in the immobilization and removal of anionic radionuclides and other compounds (Gu et al., 2018; Sakr et al., 2018). Among those applications the removal of Cr(VI) from water is relevant, this last one, in fact, is one of the most warrying pollutants for humans (Aigbe and Osibote, 2020). Different methods can be used for chromium capture and ion exchange is considered one of the best options, combining cost-effectiveness and high efficiency (Peng and Guo, 2020). Until now the most important commercially used materials for this task are the ionic exchange resins that show, as the main problem, to be susceptible of degradation and to the influence of pH while using (Marcu et al., 2021). To overcome this issue LDHs seems to be the perfect candidates, being stable in a wide pH range; a lot of experiments were done in this direction and several compositions of LDH were found to be very performing, in particular MgAl based LDH with its easy synthesis (Zeng et al., 2022). To satisfy the specific needs, considerable efforts have been made to design LDH with characteristics dedicated to the different applications (Li et al., 2022). First, there is a great variety of choices for the two cationic metals, with a consequent wide range of structural, physical and chemical properties (Naseem et al., 2019; Tang et al., 2020); secondly, the repetition of interlayer domains allows to design solids with a large surface/volume ratio; moreover, LDHs can host and exchange metal ions of mixed valence, water molecules and relatively complex organic molecules, intercalated in the interlayer space (Asiabi et al., 2017).

1.1. Purpose of the work

In contemporary discussions on water purification, it must be inevitably addressed the entire proposed process, taking into account factors such as environmental impact assessment (EIA) (Fuentes-Bargues, 2018) and adherence to the Sustainable Development Goals outlined in the United Nations 2030 Agenda, with a particular emphasis on Goal 6: Clean Water and Sanitation.

One of the most worrying problems for the latter is the disposal of spent material (rich in chromium), so it is vital to find a possible application according to the circular economy statements (Li et al., 2021). Among the different metals and anions combination to build up a LDH compound the choice of Ni(II), Fe(III) and nitrate is based on the project to reuse the LDH after the adsorption process in electrochemistry

* Corresponding author.
E-mail address: cardinal@chimica.unige.it (A. Maria Cardinale).

https://doi.org/10.1016/j.rsurfi.2024.100242
Received 20 February 2024; Received in revised form 6 June 2024; Accepted 7 June 2024
Available online 15 June 2024

applications. Basing on previous studies (Fortunato et al., 2024) the NiFe based LDH are promising in this fields, offsetting the use of elements such as nickel and iron with the possibility of a second life for the compound after the absorption of chromium.

In this study was synthesized and characterized the $[Ni_{0,66}Fe_{0,33}(OH)_2](NO_3)_{0,33}$ LDH compound, to study the best working conditions regarding the LDH adsorption of chromate ions in aqueous solution. The adsorption tests as a function of the various parameters studied (pH, contact time between the solid and the aqueous solution containing Cr(VI), initial concentration range of Cr(VI) and the ratio between the mass of LDH used and the volume of aqueous solution) were performed using the experimental design approach, allowing a detailed investigation of the effects of multiple factors on the desired response.

In a previous work (Cardinale et al., 2023)a similar investigation procedure was applied to a MgAl–NO_3 LDH to test the chromium adsorbance capacity. For the purpose to reuse the spent material (after adsorption LDH) in this work a NiFe LDH compound was tested as adsorber. Iron has well known electroactive properties, while nichel demonstrated to be electroactive (Fortunato et al., 2024), as interlayered was selected the nitrate anion due to its not interferent behavior, both in water solution and in lithium or post lithium batteries.

This material, after the adsorption, is rich in nickel, iron, and chromium; all these metals are known as electrochemically active (Ahmed and Nabi, 2021; Yang et al., 2018; Zysler et al., 1994) and for this reason it can be very interesting for energy related applications.

For an efficient reusage of the spent LDH the knowledge of the chemical-physical adsorption mechanisms is essential (Consani et al., 2018). As the adsorption mechanism the most accredited hypotheses are those of Cavani et al. (Cavani et al., 1991), i.e. the simple exchange in the interlayer of anionic compounds, and of Wang and Gao (2006), i.e. an interlayer exchange followed by adsorption on the surface of LDH. For this reason, has been discriminated the two main processes involved in the chromium adsorption, interlayer exchange and entrapment in the external octahedral cages. The optimization of the adsorption procedure, together with the knowledge of the mechanisms underlying the adsorption itself, allow to improve the technological applications of LDH NiFe–NO_3 in a broad range of fields, such as the environmental and industrial ones.

2. Materials and methods

2.1. Chemicals

All chemicals were bought and utilized without additional processing. The starting reactants for the LDH synthesis were supplied by VWR CHEMICALS, Leuven-Belgium: $Fe(NO_3)_3{\cdot}6H_2O$ (98.8% purity), $Ni(NO_3)_2{\cdot}6H_2O$ (98.9 mass% purity) and NaOH (>98 mass% purity). For the chromium-adsorption experiments anhydrous potassium chromate (K_2CrO_4 > 99.0 mass% purity) were dissolved in water to obtain stock solutions at chromate concentration of 1000 mg L^{-1}, 1,5-Diphenylcarbazide ($C_{13}H_{14}N_4O$), acetone and sulfuric acid (H_2SO_4, 95–98 mass%) were all supplied by Sigma-Aldrich Co., LLC (St. Louis, MO, USA). All aqueous solutions were freshly prepared using deionized water generated from a water purification system, at the point of use (M3/M6 Chemical Bürger s. a.s, Genova, Italy).

2.2. LDH synthesis procedure

The synthesis of NiFe–NO_3 with a molar Ni/Fe ratio of 2 has been carried out following the Boclair and Braterman (1999) method of co-precipitation. The whole synthesis needs to be performed in an CO_2 protected environment. The elimination of any form of carbonates is important because it is akin with the interlayers of the LDH. The two metallic salts were dissolved in deionized water, previously heated until boiling for about 5 min to remove carbon dioxide, while the sodium hydroxide solution was decarbonated by blowing nitrogen for about 10 min. In a three-neck flask, containing the two nitrate solutions, under mechanical stirring, the NaOH 1 M was slowly added through a drip funnel. In addition, during the reaction, the equipment set up was insulated at the best from the environment. Under the above reaction conditions, the two metallic hydroxides formed were converted to the LDH precursor according to the reaction (1):

$$Fe(OH)_{3(s)} + Ni(OH)_{2(s)} + NO_{3(aq)}^{-} \rightleftarrows [NiFe(OH)_2]NO_{3(s)} + 3\ OH_{(aq)}^{-} \text{(eq.1)}$$

At the end of the precipitation process, the pH was 13. The contents of the flask (the LDH precursor with its surnatant liquid) were subsequently transferred into a dark glass bottle and placed inside a stove at 70 °C for 48 h. During this digestion process LDH was formed. To isolate the solid from the supernatant solution several centrifugations were carried out at 5000 rfc for 5 min each, washing the precipitate each time with new decarbonated deionized water, the pH after the last wash is 7. The LDH was dried in the stove at 70 °C for 24 h. After drying the solid was pulverized with a mortar and sieved with a sieve of 120 mesh. The yield was about 70%.

2.3. Characterization

The structural properties and the composition of the synthesized samples were studied by the following techniques: X-ray analysis on powders (XRPD), Field Emission Scanning Electron Microscope analysis (FESEM) and FT-InfraRed Spectroscopy (FT-IR). X-ray powder diffraction was performed, on the samples grounded in agata mortar, with a vertical diffractometer X'Pert MPD (Philips, Almelo, The Netherlands) equipped with a Cu tube (Kα1 wavelength: 1.54 Å). The patterns were collected in a 2θ range 10°–100°, applying a scanning rate of 0.001° and measuring time of 50 s/step.

The obtained diffraction data were indexed by comparing them with existing literature or calculated data (Villarks and Cenzual, 2017), whereas the lattice parameters of the LDHs were calculated using the program LATCON (King et al., 2000). A FESEM analysis was performed to investigate the samples morphology. The samples, after being adhered on a conductive sample holder, have been analyzed applying an acceleration voltage of 5 kV for 50s, and a cobalt standard was employed for calibration. FT-IR spectra were obtained within the typical wavelength range of 4000 to 600 cm^{-1}, using a Spectrum 65 FT-IR Spectrometer (PerkinElmer, Waltham, MA, USA) featuring a KBr beam-splitter and a DTGS detector. An ATR accessory with a diamond crystal was utilized for the measurements. To determine the concentrations of the residual Cr(VI) in post-adsorption solutions and subsequently for the determination of nitric nitrogen the UV-VIS spectroscopy has been used, the instrument was a Varian Cary 50 Scan UV/VIS spectrophotometer. To measure the Cr(VI) concentration the 1,5-diphenylcarbazide method is used (Petala et al., 2013), while for the nitric nitrogen the analytical procedure followed was the one proposed by (Monteiro et al., 2003). Data analysis for the experimental designs was conducted using 'R,' the open-source software environment for statistical computing and graphics (R Core Team, 2014), with the additional package CAT (Chemometric Agile Tool) by Leardi et al. (Leardi and Melzi, 2017).

2.4. Adsorption tests experimental design

The chromate adsorption tests have been planned using an experimental design (or design of experiments, DOE). This approach, increasingly widespread in this field (Machrouhi et al., 2022; Hosseini et al., 2022; Behbahani et al., 2021; Sayed et al., 2020), consists in the study of the effect of multiple variables at the same time, making it much more convenient than the classic univariate approach for several reasons: (i) by applying multiple regression techniques, it takes into account the interactions among the variables; (ii) it requires fewer experimental runs; (iii) it allows to obtain empirical mathematical

relationships between the variables and the response (Benedetti et al., 2022).

To investigate the adsorption properties and effectiveness of the LDHs concerning Cr(VI), the chosen parameters (or factors) to be investigated were the ratio mass of LDH/solution volume, the pH, the initial concentration of Cr(VI) and the mixing time between the solid and the chromate solution. For each factor, the experimental domain (i.e. the minimum and maximum values) were set by taking into consideration tests carried out in previous work (Cardinale et al., 2022). However, to choose the values of initial concentration of Cr(VI), a preliminary univariate screening was performed, changing the Cr(VI) concentration from 5 ppm to 140 ppm at a mass of LDH/solution volume of 1 g/L. Each test has been conducted by placing the LDH and the solution on a rotating stirrer for 2 h. After mixing the samples were centrifuged to separate the LDH from the solution, the solid recovered has been analyzed by PXRD to check any changing in the crystal structure, while the residual solution was analyzed by UV-VIS with the diphenylcarbazide method to determine the residual concentration of CrO_4^{2-} ions in the solution. This preliminary test results in a variable absorption capacity, with an absorption range of between 12 and 20 ppm.

The selected DOE for the adsorption tests was the Doehlert (Benedetti et al., 2022), a response surface design which allows to build a quadratic model of the response as a function of the variables. In particular, this design is able to explore the k factors at different number of levels: in this study (k = 4), one factor is studied at 3 levels, one at 5 and two at 7. A total of 42 experiments were performed, consisting of two distinct replicates of 21 conditions (Table 1). To minimize the influence of systematic trends, the experiments were performed randomly.

3. Experimental results and discussion

3.1. Characterization

Prior to be used for adsorption purposes the synthesized LDH has been characterized focusing on the crystal structure, the composition and the morphology. Fig. 1a) shows the PXRD pattern which confirms the typical turbostratic LDH structure (space group R-3m), with the characteristic symmetric diffraction peaks (003) at 11.3°, (006) at 22.5°, (009) at 33.8°, and the asymmetric "fin-like" ones (102) at 34.6°, (105) at 38.7°, (108) at 45.8° and (110) at 60.0°. The cell parameters are a = b = 0.3075 nm, c = 2.3350 nm and the interlayer region, calculated as suggested by Conterosito et al. (2013), is approximately 0.30 nm.

The FTIR spectrum in Fig. 1b) reveals the O–H stretching vibrations of the hydroxyl groups and the presence of water molecules in the interlayer of LDH (the intense and broad adsorption band centered at about 3370 cm^{-1}), this band results from the overlapping of the O–H bond stretching of both the hydroxyl groups (at 3300 cm^{-1}) and interlayered lattice water bonded with the transition metals (2850 cm^{-1}).

Ongoing through the lower wavenumbers the band at 1620 cm^{-1} is due to the bending of water and at 1460 cm-1 there is a slight shoulder related to a small amount of undesired carbonate anion, unavoidable even if the synthesis was carried out in an inert atmosphere. At 1330 cm^{-1} a sharp characteristic absorption band, corresponding to the stretching vibration mode of NO_3^-, confirms the nitrate anion in the interlayer of the synthetized LDH.

The morphology of the material is depicted in the FESEM image (Fig. 2). The material is homogeneous and characterized by a columnar structure formed from multiple layers of compound that are slightly misaligned, such structure is typical of turbostratic materials like LDH synthesized through co-precipitation.

Table 1
Experimental conditions of the Doehlert design for the first performed adsorption tests.

Experiment	*LDH/ solution (g/L)*	*Equilibration time (min)*	*Cr(VI) concentration (ppm)*	pH	*Adsorption Rate (%)*
1	*5.50*	*60.0*	*40.0*	*7.0*	*100.0*
2	*10.00*	*60.0*	*40.0*	*7.0*	*100.0*
3	*7.75*	*86.0*	*40.0*	*7.0*	*100.0*
4	*7.75*	*68.7*	*56.3*	*7.0*	*100.0*
5	*7.75*	*68.7*	*44.1*	*9.0*	*100.0*
6	*1.00*	*60.0*	*40.0*	*7.0*	*50.0*
7	*3.25*	*34.0*	*40.0*	*7.0*	*97.0*
8	*3.25*	*51.3*	*23.7*	*7.0*	*100.0*
9	*3.25*	*51.3*	*35.9*	*5.0*	*99.7*
10	*7.75*	*34.0*	*40.0*	*7.0*	*100.0*
11	*3.25*	*86.0*	*40.0*	*7.0*	*96.5*
12	*7.75*	*51.3*	*23.7*	*7.0*	*100.0*
13	*3.25*	*68.7*	*56.3*	*7.0*	*92.3*
14	*7.75*	*51.3*	*35.9*	*5.0*	*100.0*
15	*3.25*	*68.7*	*44.1*	*9.0*	*71.7*
16	*5.50*	*77.3*	*23.7*	*7.0*	*99.7*
17	*5.50*	*42.7*	*56.3*	*7.0*	*99.9*
18	*5.50*	*77.3*	*35.9*	*5.0*	*99.9*
19	*5.50*	*42.7*	*44.1*	*9.0*	*99.7*
20	*5.50*	*60.0*	*52.3*	*5.0*	*100.0*
21	*5.50*	*60.0*	*27.7*	*9.0*	*100.0*

3.2. Adsorption

As the chromium adsorption measurements, the acquired data were subsequently analyzed through multiple regression tests using the CAT software (see Materials and Methods), producing a mathematical model capable of describing the concentration of (Cr(VI) adsorbed as a function of the four factors under evaluation in the interesting domain (Eq 1). Overall, the obtained model showed an excellent fitting, able to explain 95.6% of the variance of the system.

$$Cr(VI)_{ads} = 7.273 - \mathbf{6.583\ R} - 0.131\ t + \mathbf{3.586\ C} - 0.515 \cdot pH + 0.036\ R\ t - \textit{2.683\ R\ C} + 2.172\ R \cdot pH + 0.328\ t\ C - 0.639\ t \cdot pH - 0.599\ C \cdot pH + 3.975 \cdot R^2 + 0.346\ t^2 + 0.030 \cdot C^2 - 0.483\ pH^2 \quad \text{(eq. 1)}$$

In the equation, R, t, C and pH are the four factors, i.e. ratio mass of LDH/solution volume, mixing time between the solid and the chromate solution, the initial concentration of Cr(VI) and pH, respectively.

Coefficients significant at the 95% confidence level are highlighted in italic, while those significant at the 99.9% confidence level are highlighted in bold.

The coefficients are also depicted in Fig. 3a, in Fig. 3b is shown the contour plot for the two more significant variables.

In this experimental domain, equilibration time and pH showed no significant effects on the response, while both the ratio LDH mass/solution volume and the initial chromium concentration demonstrated significant and robust influences (99.9% confidence level) and interaction (95% confidence level). In particular, the amount of adsorbed Cr (VI) increases by decreasing the LDH mass/volume and by increasing Cr concentration (Fig. 3b).

To deeper investigate the relationships among the adsorption efficiency and the two more relevant parameters, a further set of measurements has been carried out following a new experimental design, extending the experimental domain to higher values of Cr(VI) concentration (range 30–90 ppm) and reducing the maximum value of the ratio LDH mass/solution volume (range 1–4 g/L).

The equilibration time and pH were maintained at 30 min and 7, respectively. The selected design was the face-centered central composite design (CCD), another response surface design which provides a quadratic model. It explores the factors at the same number of levels for all the factors, i.e. three (−1, 0, +1). A total of 12 experiments were performed, consisting of 8 conditions at the vertices of the domain and 4 replicates of condition 9, i.e. the center point (Table 2). Also, in this case the experiments were performed randomly, however four replicates of the center point were consistently conducted throughout the analysis sequence to provide an estimate of the experimental variance.

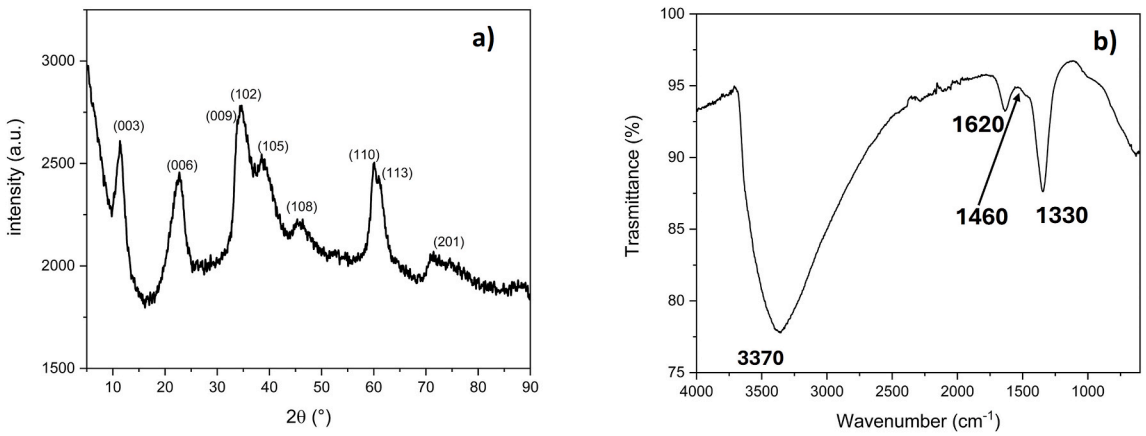

Fig. 1. a) XRD powder pattern of NiFe-nitrate LDH. b) FT-IR spectrum of the NiFe-nitrate LDH.

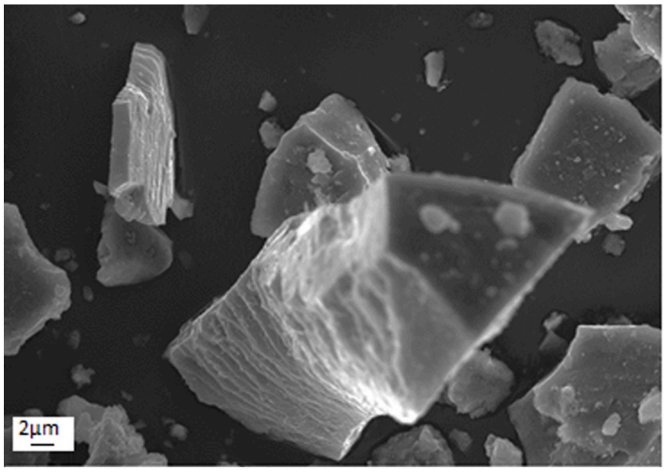

Fig. 2. FE-SEM image of the NiFe–NO_3 LDH.

After data elaboration, a mathematical model with an explained variance of 94.7% was obtained, using equation (2):

$$Cr(VI)_{ads} = 14.656 - 2.002\,R + 3.188\,C + 0.903\,R\,C + 0.080 \cdot R^2 - 0.781 \cdot C^2 \quad \text{(eq. 2)}$$

The coefficients plot and the response surface are reported in Fig. 4a and b, respectively. The results in this experimental domain confirm the findings obtained with the first DOE, with strong opposite influences of the two factors, which also interact with each other. However, when expressing the response as a percentage of adsorbed Cr(VI), the trend is the opposite (Fig. 4c).

The results demonstrate that a high quantity of NiFe–NO_3 LDH reaches saturation in an environment with a low concentration of Cr(VI) but, conversely, the ratio Cr(VI) adsorbed/LDH mass highly increases when operating with a lower LDH ratio in a solution with a high concentration of chromate ions.

To determine the saturation point, as the maximum quantity of chromium adsorbed by 1 g/L of LDH, at pH = 7 and a mixing time of 30 min, a new set of measurements were carried out under the aforementioned conditions, by varying the concentration of Cr(VI) in the range of 12–90 ppm. In Fig. 5 is reported the adsorption trend, that follows a regular pattern up to 40 ppm of chromium starting concentration,

Table 2
Experimental conditions of the CCD for the second performed adsorption tests.

Experiment	LDH/solution (g/L)	Cr(VI) concentration (ppm)	Adsorption Rate (%)
1	*1*	*30*	*47.3*
2	*4*	*30*	*100.0*
3	*1*	*90*	*20.6*
4	*4*	*90*	*68.7*
5	*4*	*60*	*91.1*
6	*2.5*	*90*	*48.1*
7	*1*	*60*	*26.5*
8	*2.5*	*30*	*87.7*
9	*2.5*	*60*	*60.0*

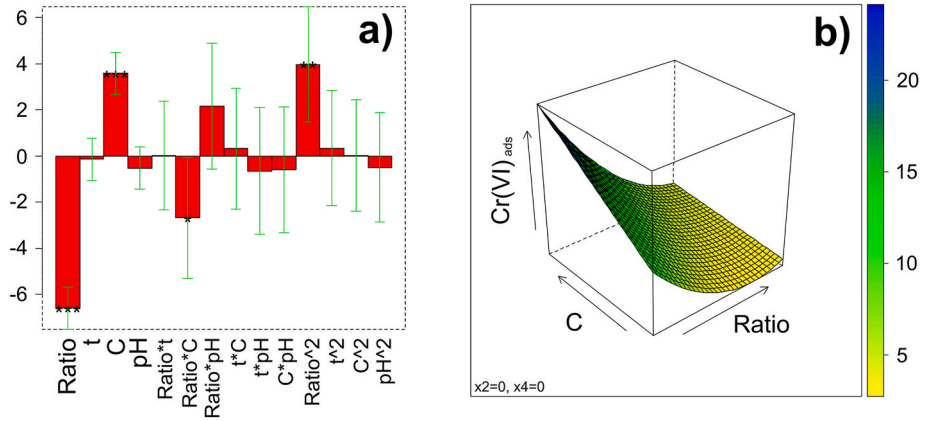

Fig. 3. (a) Coefficient significance of the Doehlert design. The error bars represent the confidence interval of the coefficients at p = 0.05. (b) 3D Contour plot for binary influence of Cr(VI) concentration vs. LDH mass/solution volume.

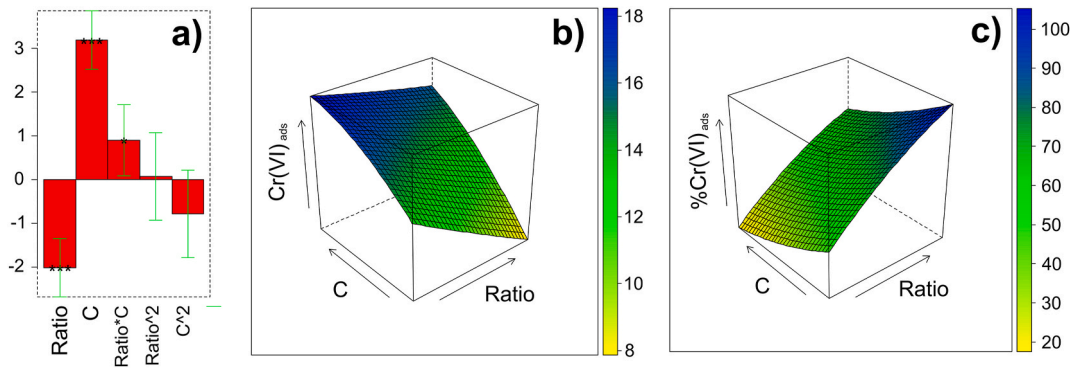

Fig. 4. (a) Coefficient significance of the central composite design. The error bars represent the confidence interval of the coefficients at p = 0.05. (b) 3D Contour plot for binary influence of Cr(VI) concentration vs. LDH mass/solution volume (response as concentration of adsorbed Cr(VI)). (c) 3D Contour plot for binary influence of Cr(VI) concentration vs. LDH mass/solution volume (response as percentage of adsorbed Cr(VI)).

followed by an irregular increase in the adsorption capability.

Moreover, the trend observed in Fig. 5 suggests a change in the mechanism of adsorption, over the initial concentration of 40 ppm, as suggested by (Wang and Gao, 2006), moving from a simple pure interlayer exchange process, in which chromate substitutes nitrate, to an absorption of the chromate anion in the external octahedral cages of the LDH hydroxyl layers.

To discriminate between the two implied adsorption mechanisms a measurement of the nitrate anion released in the solution after the adsorption process has been carried out. Nitrogen, in solution after the adsorption process, has been measured under saturation conditions or rather a ratio solid/solution 1 g/L and a chromium initial concentration ranging from 30 ppm to 80 ppm. All the tests have been carried out in duplicate. Table 3 reports the results and Fig. 6 shows the ratio between the nitrogen released and chromium adsorbed Vs the initial chromium concentration.

At an initial chromium amount of 30 ppm the quantity of the released nitrogen is almost twice the amount of Cr(VI) adsorbed, as expected with the hypothesized interlayer exchange mechanism in which one divalent chromate anion substitutes two monovalent nitrate anions. Increasing the amount of chromium in the solution the adsorption results show a very slow increasing while the nitrogen released doesn't change appreciably, consequently the ratio slowly decreases (Fig. 6), this is accordance with literature (Wang and Gao, 2006) and

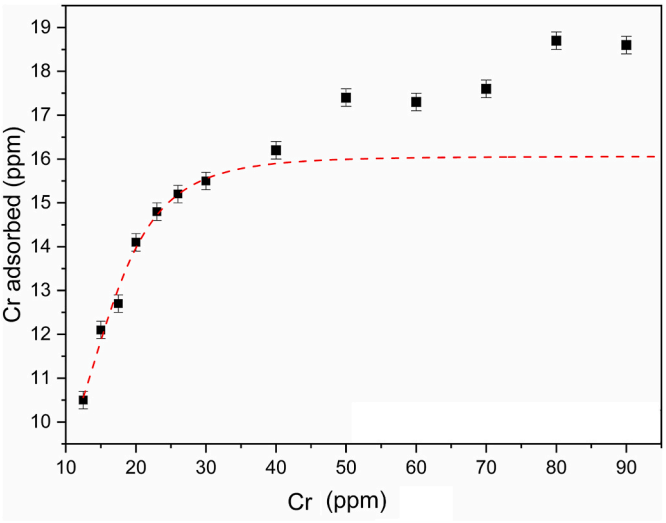

Fig. 5. Concentration of chromium adsorbed vs chromium initial concentration. The dotted line extrapolates the regular increase in the adsorption. The error bars represent the standard deviation of the measurements (n = 2).

Table 3
Nitrogen released in solution after chromium adsorption and ratio between the two values.

Cr initial concentration		Cr adsorbed concentration	N released	N released/Cr adsorbed
ppm	mM	mM	mM	mM/mM
30	0.58	0.30	0.58	*1.93*
40	0.77	0.31	0.55	*1.77*
50	0.96	0.35	0.57	*1.63*
60	1.15	0.33	0.56	*1.71*
70	1.35	0.34	0.56	*1.64*
80	1.54	038	0.60	*1.58*

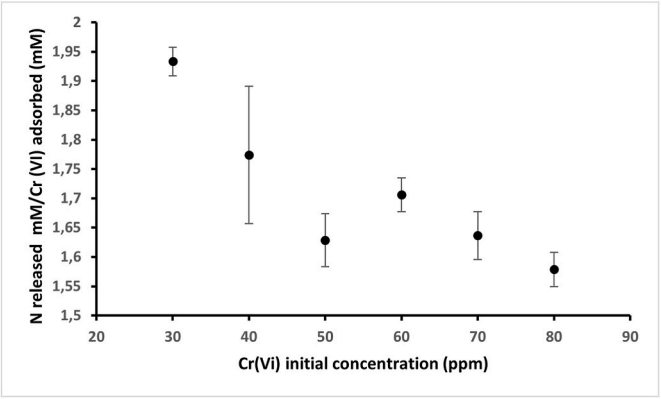

Fig. 6. Nitrogen released in the solution after the adsorption process vs chromium adsorbed at different initial concentration. The error bars represent the standard deviation of the measurements (n = 2).

suggests that up to a concentration of about 30 ppm chromium (near to the adsorbance plateau in Fig. 5) the adsorption can be ascribed to a simple interlayer mechanism, while increasing the initial Cr(VI) amount and approaching to the saturation condition the further chromium adsorbed is attributable to a insertion in an external cage space.

The results in Fig. 5 reveal that at an initial concentration of 40 ppm of chromium the interlayer exchange saturation point has been almost reached and, in these conditions, the adsorption capacity q_e can be calculated by equation (2))

$$q_e = V(c_0 - c_e) / m \quad (2)$$

Here, m denotes the mass of sorbent utilized in a liquid hold-up volume V, c_0 denotes the initial concentration (mg/L) of the pollutant, and *ce* indicates the chromium concentration in the liquid phase in equilibrium

with the chromium adsorbed in the solid phase at concentration *qe*. At 40 ppm concentration qe = 16 mg/g.

The removal rate r, specifically, the percentage of solid adsorbed relative to the initial concentration, can be written as:

$r = ((c_0 - c_e)/c_0)$ x 100 and assumes the value r = 40.

The adsorption performance of the NiFe LDH can be evaluated against that examined by (Zheng et al., 2019). Despite they consist in the same cations, but are still different as concern the anions, a comparison deserves to be made. In similar saturation conditions the LDH studied by (Zheng et al., 2019) shows a qe of about 30 mg/g, that is slightly higher than the one studied in this work. This result is offset by the reusage in electrochemical application if the interlayered anion is nitrate.

4. Conclusions

A NiFe-nitrate LDH was synthesized and characterized to be tested as a Cr(VI) adsorbent for remediation purposes. The experimental design was employed to optimize the configuration of the experimental measurements. The physicochemical interactions between the LDH and the chromate anion were examined, to discriminate between two different capture processes. According with the experimental results, the following conclusions can be drawn:

- The synthesis of NiFe-nitrate LDH is straightforward and can be reproduced consistently.
- Incorporating an experimental design (DOE) in the measurement setup significantly reduces the number of experimental tests required, enabling a comprehensive understanding of the entire system's behavior.
- The maximum adsorption capacity is 16.0 mg/g at neutral pH conditions.
- As the influence of the different adsorption parameters investigated, as predicted, the chromium adsorption increases for high LDH/solution volume ratios and low concentrations of Cr(VI).
- For this LDH the adsorption mechanism, which can be inferred from the experimental results, consists of two different processes, an interlayer anionic exchange (predominant up to the saturation point) and an entrapment of the chromate from the solution to the external octahedral cages.

Funding sources

This research did not receive any specific grant from funding agencies in the public, commercial, or not-for-profit sectors.

CRediT authorship contribution statement

Anna Maria Cardinale: Writing – review & editing, Writing – original draft, Supervision, Resources, Conceptualization. **Marco Fortunato:** Writing – review & editing, Investigation, Formal analysis, Data curation. **Francisco Ardini:** Writing – review & editing, Writing – original draft, Validation, Software, Methodology, Conceptualization.

Declaration of competing interest

The authors declare that they have no known competing financial interests or personal relationships that could have appeared to influence the work reported in this paper.

Data availability

Data will be made available on request.

References

Ahmed, R., Nabi, G., 2021. Enhanced electrochemical performance of Cr-doped NiO nanorods for supercapacitor application. J. Energy Storage 33, 102115. https://doi.org/10.1016/J.EST.2020.102115.

Aigbe, U.O., Osibote, O.A., 2020. A review of hexavalent chromium removal from aqueous solutions by sorption technique using nanomaterials. J. Environ. Chem. Eng. 8, 104503 https://doi.org/10.1016/J.JECE.2020.104503.

Asiabi, H., Yamini, Y., Shamsayei, M., 2017. Highly selective and efficient removal of arsenic(V), chromium(VI) and selenium(VI) oxyanions by layered double hydroxide intercalated with zwitterionic glycine. J. Hazard Mater. 339, 239–247. https://doi.org/10.1016/j.jhazmat.2017.06.042.

Behbahani, E.S., Dashtian, K., Ghaedi, M., 2021. Fe3O4-FeMoS4: promise magnetite LDH-based adsorbent for simultaneous removal of Pb (II), Cd (II), and Cu (II) heavy metal ions. J. Hazard Mater. 410 https://doi.org/10.1016/j.jhazmat.2020.124560.

Benedetti, B., Caponigro, V., Ardini, F., 2022. Experimental design step by step: a practical guide for beginners. Crit. Rev. Anal. Chem. 52, 1015–1028.

Boclair, J.W., Braterman, P.S., 1999. Layered double hydroxide stability. 1. Relative stabilities of layered double hydroxides and their simple counterparts. Chem. Mater. 11, 298–302. https://doi.org/10.1021/cm980523u.

Cardinale, A.M., Carbone, C., Fortunato, M., Fabiano, B., Pietro Reverberi, A., 2022. ZnAl-SO4 layered double hydroxide and allophane for Cr(VI), Cu(II) and Fe(III) adsorption in wastewater: structure comparison and synergistic effects. Materials 15. https://doi.org/10.3390/ma15196887.

Cardinale, A.M., Carbone, C., Molinari, S., Salviulo, G., Ardini, F., 2023. MgAl-NO3 LDH: adsorption isotherms and multivariate optimization for Cr(VI) removal. Chemistry (Switzerland) 5, 633–645. https://doi.org/10.3390/chemistry5010045.

Cavani, F., Trifirò, F., Vaccari, A., 1991. Hydrotalcite-type anionic clays: preparation, properties and applications. Catal. Today 11, 173–301. https://doi.org/10.1016/0920-5861(91)80068-K.

Consani, S., Balić-Žunić, T., Cardinale, A.M., Sgroi, W., Giuli, G., Carbone, C., 2018. A novel synthesis routine for woodwardite and its affinity towards light (La, Ce, Nd) and heavy (Gd and Y) rare earth elements. Materials 11. https://doi.org/10.3390/ma11010130.

Conterosito, E., Croce, G., Palin, L., Pagano, C., Perioli, L., Viterbo, D., Boccaleri, E., Paul, G., Milanesio, M., 2013. Structural characterization and thermal and chemical stability of bioactive molecule-hydrotalcite (LDH) nanocomposites. Phys. Chem. Chem. Phys. 15, 13418–13433. https://doi.org/10.1039/c3cp51235e.

Fortunato, M., Pietro Reverberi, A., Fabiano, B., Cardinale, A.M., 2024. Thermal evolution of NiFe-NO3 LDH and its application in energy storage systems. Energies 17. https://doi.org/10.3390/en17051035.

Fuentes-Bargues, J.L., 2018. Review of the environmental impact assessment process of wastewater treatment plants in Spain. Environ. Protect. Eng. 44, 23–41. https://doi.org/10.5277/epe180402.

Gu, P., Zhang, S., Li, X., Wang, X., Wen, T., Jehan, R., Alsaedi, A., Hayat, T., Wang, X., 2018. Recent advances in layered double hydroxide-based nanomaterials for the removal of radionuclides from aqueous solution. Environ. Pollut. 240, 493–505. https://doi.org/10.1016/j.envpol.2018.04.136.

Hosseini, O., Zare-Shahabadi, V., Ghaedi, M., Azqhandi, M.H.A., 2022. Experimental design, RSM and ANN modeling of tetracycline photocatalytic degradation using LDH@CN. J. Environ. Chem. Eng. 10 https://doi.org/10.1016/j.jece.2022.108345.

Jiehu, C., Chunlei, W., Ming, Z., Jie, Z., Li, F., Xiuhong, D., Leiming, C., Chunguang, L., 2020. 2D to 3D controllable synthesis of three Zn-Co-LDHs for rapid adsorption of MO by TEA-assisted hydrothermal method. Appl. Surf. Sci. 534 https://doi.org/10.1016/j.apsusc.2020.147564.

King, G., Schwarzenbach, L., 2000. In: Hall, S.R., du Boilay, D.J. (Eds.), Xtal3.7 System. Olthof-Hazekamp R.

Leardi, R., Melzi, C., 2017. G. Polotti, CAT(Chemometric Agile Tool).

Lei, C., Zhu, X., Zhu, B., Jiang, C., Le, Y., Yu, J., 2017. Superb adsorption capacity of hierarchical calcined Ni/Mg/Al layered double hydroxides for Congo red and Cr(VI) ions. J. Hazard Mater. 321, 801–811. https://doi.org/10.1016/j.jhazmat.2016.09.070.

Li, M., Chowdhury, T., Kraetz, A.N., Jing, H., Dopilka, A., Farmen, L.M., Sinha, S., Chan, C.K., 2019. Layered double hydroxide sorbents for removal of selenium from power plant wastewaters. Chem Eng 3, 1–24. https://doi.org/10.3390/chemengineering3010020.

Li, X., Fortunato, M., Cardinale, A.M., Sarapulova, A., Njel, C., Dsoke, S., 2021. Electrochemical study on nickel aluminum layered double hydroxides as high-performance electrode material for lithium-ion batteries based on sodium alginate binder. J. Solid State Electrochem. https://doi.org/10.1007/s10008-021-05011-y.

Li, K., Li, S., Li, Q., Liu, H., Yao, W., Wang, Q., Chai, L., 2022. Design of a high-performance ternary LDHs containing Ni, Co and Mn for arsenate removal. J. Hazard Mater. 427 https://doi.org/10.1016/j.jhazmat.2021.127865.

Machrouhi, A., Taoufik, N., Elhalil, A., Tounsadi, H., Rais, Z., Barka, N., 2022. Patent blue V dye adsorption by fresh and calcined Zn/Al LDH: effect of process parameters and experimental design optimization. Journal of Composites Science 6. https://doi.org/10.3390/jcs6040115.

Marcu, C., Balla, A., Szűcs Balázs, J.Z., Lar, C., 2021. Adsorption isotherms and thermodynamics for chromium (VI) using an anion exchange resin. Anal. Lett. 54, 1783–1793. https://doi.org/10.1080/00032719.2020.1825464.

Monteiro, M.I.C., Ferreira, F.N., De Oliveira, N.M.M., Ávila, A.K., 2003. Simplified Version of the Sodium Salicylate Method for Analysis of Nitrate in Drinking Waters.

Naseem, S., Gevers, B., Boldt, R., Labuschagné, F.J.W.J., Leuteritz, A., 2019. Comparison of transition metal (Fe, Co, Ni, Cu, and Zn) containing tri-metal layered double hydroxides (LDHs) prepared by urea hydrolysis. RSC Adv. 9, 3030–3040. https://doi.org/10.1039/c8ra10165e.

Peng, H., Guo, J., 2020. Removal of chromium from wastewater by membrane filtration, chemical precipitation, ion exchange, adsorption electrocoagulation, electrochemical reduction, electrodialysis, electrodeionization, photocatalysis and nanotechnology: a review. Environ. Chem. Lett. 18, 2055–2068. https://doi.org/10.1007/s10311-020-01058-x.

Petala, E., Dimos, K., Douvalis, A., Bakas, T., Tucek, J., Zbořil, R., Karakassides, M.A., 2013. Nanoscale zero-valent iron supported on mesoporous silica: characterization and reactivity for Cr(VI) removal from aqueous solution. J. Hazard Mater. 261, 295–306. https://doi.org/10.1016/j.jhazmat.2013.07.046.

R Core Team, 2014. A Language and Envinromentfor Statistical Computing. R Foundation for Statistical Computing.

Sakr, A.A.E., Zaki, T., Elgabry, O., Ebiad, M.A., El-Sabagh, S.M., Emara, M.M., 2018. Mg-Zn-Al LDH: influence of intercalated anions on CO2 removal from natural gas. Appl. Clay Sci. 160, 263–269. https://doi.org/10.1016/j.clay.2018.02.043.

Sayed, M.R., Abukhadra, M.R., Abdelkader Ahmed, S., Shaban, M., Javed, U., Betiha, M. A., Shim, J.J., Rabie, A.M., 2020. Synthesis of advanced MgAl-LDH based geopolymer as a potential catalyst in the conversion of waste sunflower oil into biodiesel: response surface studies. Fuel 282. https://doi.org/10.1016/j.fuel.2020.118865.

Tang, Z., Qiu, Z., Lu, S., Shi, X., 2020. Functionalized layered double hydroxide applied to heavy metal ions absorption: a review. Nanotechnol. Rev. 9, 800–819. https://doi.org/10.1515/ntrev-2020-0065.

Thite, V.D., Giripunje, S.M., 2022. Adsorption and photocatalytic performance of ZnAl layered double hydroxide nanoparticles in removal of methyl orange dye. Nanotechnology for Environmental Engineering 7. https://doi.org/10.1007/s41204-021-00186-1.

Villarks, P., Cenzual, K., 2017. Pearson's Crystal Data- Crystal Structure Database for Inorganic Compounds.

Wang, Y., Gao, H., 2006. Compositional and structural control on anion sorption capability of layered double hydroxides (LDHs). J. Colloid Interface Sci. 301, 19–26. https://doi.org/10.1016/j.jcis.2006.04.061.

Yang, C.C., Zhang, D.M., Du, L., Jiang, Q., 2018. Hollow Ni-NiO nanoparticles embedded in porous carbon nanosheets as a hybrid anode for sodium-ion batteries with an ultra-long cycle life. J Mater Chem A Mater 6, 12663–12671. https://doi.org/10.1039/c8ta03692f.

Zeng, B., Wang, Q., Mo, L., Jin, F., Zhu, J., Tang, M., 2022. Synthesis of Mg-Al LDH and its calcined form with natural materials for efficient Cr(VI) removal. J. Environ. Chem. Eng. 10, 108605 https://doi.org/10.1016/J.JECE.2022.108605.

Zheng, Y., Cheng, B., You, W., Yu, J., Ho, W., 2019. 3D hierarchical graphene oxide-NiFe LDH composite with enhanced adsorption affinity to Congo red, methyl orange and Cr(VI) ions. J. Hazard Mater. 369, 214–225. https://doi.org/10.1016/j.jhazmat.2019.02.013.

Zysler, R., Fiorani, D., Dormann, J.L., Testa, A.M., 1994. Magnetic properties of ultrafine α-Fe2O3 antiferromagnetic particles. J. Magn. Magn Mater. 133, 71–73. https://doi.org/10.1016/0304-8853(94)90492-8.